UNIVERSITAT POLITÈCNICA DE CATALUNYA BARCELONATECH

UPCommons

Portal del coneixement obert de la UPC

http://upcommons.upc.edu/e-prints

Aquesta és una còpia de la versió *author's final draft* d'un article publicat a la revista *Energy and buildings.*

URL d'aquest document a UPCommons E-prints:

http://hdl.handle.net/2117/106990

Article publicat / *Published paper*:

Tejedor, B., Casals, M., Gangolells, M., Roca, X. (2017). Quantitative internal infrared thermography for determining in-situ thermal behaviour of façades. *Energy and buildings*, 151: 187-197. DOI: 10.1016/j.enbuild.2017.06.040.

© 2017. This manuscript version is made available under the CC-BY-NC-ND 3.0 license http://creativecommons.org/licenses/by-nc-nd/3.0/

Tejedor B., Casals M., Gangolells M., Roca X. Quantitative internal infrared thermography for determining in-situ thermal behaviour of façades. *Energy and Buildings*, 2017, 151C: 187-197. <doi: 10.1016/j.enbuild.2017.06.040>.

Final version available at:
< http://www.sciencedirect.com/science/article/pii/S0378778817301305>

Quantitative internal infrared thermography for determining in-situ thermal behaviour of façades

Blanca Tejedor, Miquel Casals, Marta Gangolells, Xavier Roca

Universitat Politècnica de Catalunya, Department of Project and Construction Engineering, Group of Construction Research and Innovation (GRIC), C/ Colom, 11, Ed. TR5, 08222 Terrassa (Barcelona), Spain

* Corresponding author: Blanca Tejedor. Tel: (+34) 93 7398919, Fax: (+34) 93 7398101. E-mail: blanca.tejedor@upc.edu

POSTPRINT

ABSTRACT

The thermal behaviour of a building is often underestimated or neglected during its construction and operation stages. In recent years, the heat flux meter (HFM) method has been commonly used to determine the U-value, a key parameter for assessing the thermal quality of the building envelope in steady-state conditions. However, this non-invasive test takes at least 72h to execute, the accuracy is 14-28%, and it is not reliable for non-homogeneous building elements. An alternative technique is based on infrared thermography (IRT). Although it is generally used for qualitative analysis, quantitative internal IRT methods may also be adopted for in-situ measurement of the U-value. This research presents a method for determining in-situ U-values using quantitative internal IRT with a deviation of 1-2% for single-leaf walls and 3-4% for multi-leaf walls. It takes 2-3 hours and can be used to provide information about the building envelope for the future refurbishment of existing buildings or to check the thermal behaviour of new building façades according to their design parameters.

Keywords:
quantitative infrared thermography (IRT), thermal transmittance (U-value), in-situ measurement, building façade, energy performance gap.

1. INTRODUCTION

In most European countries, residential buildings represent around 40% of the primary energy consumption [1-3]. In order to reduce the energy dependency and improve energy performance of buildings, two European Directives have been enforced. Directive 2010/31/EU [4] on the energy performance of buildings

requires energy certification for properties to achieve higher energy savings and guarantee adequate indoor comfort conditions for users [5,6]. Directive 2012/27/EU [7] on the energy efficiency establishes a set of binding measures to use energy more efficiently at all stages of the energy chain. These directives have forced public administrations, designers, private companies and building manufacturers to ensure the minimum energy performance gap, which is the same as the minimum possible deviation between the designed and the real building energy performance [8,5,9]. The main factors that contribute to the energy performance gap are a lack of testing before delivering a building to a user and post-occupancy monitoring. Building elements may not perform as expected when they are in situ [8-13]. A thorough literature review showed that the thermal behaviour of a building is often underestimated or neglected during its construction and operation stages [9, 11, 13, 10, 14, 15].

The U-value has become a key parameter for assessing the thermal quality of the building envelope and steady-state heat transmission performance [16,17]. Nevertheless, the measured thermal transmittance in real buildings can be rather different from that estimated by modelling and calculations [12,6]. Albatici et al. [18] and Gaspar et al. [19] highlighted that in-situ U-values are commonly determined by the heat flux meter (HFM) method according to ISO 9869-1:2014 [20]. The HFM consists of monitoring the heat flux rate passing through the façade and the indoor and outdoor environmental temperatures to obtain the thermal transmittance. However, this method presents some limitations. The first is that the HFM can only measure a local point of the wall. Therefore, it does not provide accurate results for non-homogenous building elements [21]. Secondly, it requires a minimum test duration of 72 hours and a maximum of one week [20]. Within this context, infrared thermography (IRT) may be a good alternative for in-situ U-value measurements. IRT is a non-destructive test based on measuring the radiant thermal energy distribution (heat) emitted from an object's surface [22]. Traditionally, IRT has only been used to detect thermal irregularities in building envelopes qualitatively, following EN 13187:1998 [23] and the RESNET Interim Guideline for Thermographic Inspections of Buildings [24]. Nevertheless, quantitative IRT methods may also be adopted to determine U-values even though they are still not fully developed [21]. In comparison with HFM, IRT allows the assessment of a wall area and only requires 2-3 hours of test duration.

Within the field of measuring on-site U-values with quantitative IRT, the main studies were conducted by Albatici and Tonelli [5], Albatici et al. [25] and Fokaides et al. [26]. Albatici and Tonelli [5] and Albatici et al. [25] took measurements from outside the building, while Fokaides et al. [26] carried out tests from inside the building. External thermography has several limitations. Firstly, it is more susceptible to environmental conditions than internal thermography, which provides a much more controlled environment with slower and less significant climatic fluctuations [26]. Secondly, many objects with unknown thermal status can reflect on the target and there is no control of the reflection index [26]. Finally, according to Dall'O et al. [27], the external convective coefficient cannot be considered constant in outside tests, and must be calculated on the basis of weather conditions to achieve an acceptable result.

POSTPRINT

Therefore, Jürge's equation can be used to determine the external convective heat transfer coefficient [5, 27, 25, 28]. This equation establishes a linear relationship between the external convective heat transfer coefficient and the wind speed. Despite being widely used in modelling, simulations and relevant calculations, Jürge's equation has several shortcomings [29]. The value of the convective heat transfer coefficient may be overestimated, and it may vary widely at different positions on the surface of a building [30-32]. In fact, surface-to-wind angle, wind intensity and wind direction play an important role, and are strongly affected by the building's surroundings [33, 27, 34]. Along this line, Albatici et al. [25] and Dall'O et al. [27] highlighted that the deviation between notional and measured U-value might be higher in light walls than in heavy walls. The impact of wind speed will be greater in elements with low thermal mass, since they cool down faster. Alternatively, the external convective heat transfer coefficient can be estimated using a tabulated value stated in UNE-EN ISO 6946:2012 [35]. However, this convective heat transfer coefficient is high, a precautionary value, since it is used to determine the heat loss during the design stage of the building façade [27].

Taking into account all the aspects mentioned above, this paper develops a quantitative internal IRT method for the in-situ measurement of U-values. UNE-EN ISO 6946:2012 [35] and ISO 9869-1:2014 [20] recommendations were used as references for the test conditions and data analysis. The method determines total thermal resistance and transmittance of a wall from inside the building envelope, using a passive approach. Assuming one dimensional and horizontal heat flux under steady-state conditions through the building façade, this proposed quantitative IRT method was found to be suitable for heavy walls, including both single-leaf and multi-leaf walls. In addition, it is more accurate than the HFM method and has a shorter execution time.

The paper is divided into the following sections. Section 2 describes the main features of the method, including the test conditions that must be considered, the elements of measuring equipment, how data acquisition and post-processing should be performed, and the determination of instantaneous and average measured U-values. Section 3 evaluates the accuracy of the method. In Section 4, two case studies are presented as examples of the application of the method. In Section 5, a comparative analysis between theoretical and measured U-values using tabulated values is done, in accordance with the regulations. In addition, other aspects related to the execution of the method are highlighted. Finally, Section 6 describes the main contributions of this research.

POSTPRINT

2. DEVELOPMENT OF THE METHOD

The method is represented in Figure 1.

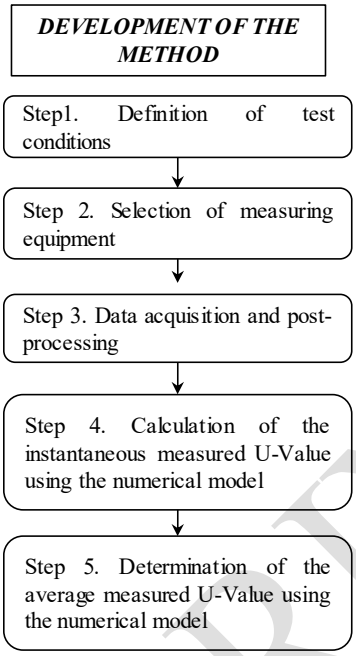

Figure 1. Flowchart of the method

2.1. Definition of test conditions

Qualitative IRT tests are defined by EN 13187:1998 [23] and the RESNET Interim Guidelines for Thermographic Inspections of Buildings [24]. Previous researchers have established boundary conditions for quantitative IRT tests [36, 30, 37, 38, 5, 39, 26, 40-43, 27, 16, 44-52, 17, 53-57, 25, 6, 58, 59, 72]. The most relevant are detailed below.

Tests should be performed under low values of wind speed. The recommendation is 0.2 to 1.0 m/s. This parameter can lead to greater thermal dispersion of convective factors.

Tests should be conducted on the northern façades of buildings and preferably in the early morning before sunrise and/or in the evening after sunset, to avoid solar radiation. Otherwise, artificial screening may be used. Incident solar radiation can be considered a kind of thermal stimulus under non-steady heat transfer conditions, which may lead to a time lag of a few hours. The wall temperature may tend to increase affecting the evaporation process in materials. In addition, incident solar radiation depends on other parameters and may not be easily predictable.

POSTPRINT

Tests must be carried out with a temperature difference (ΔT) across the building façade of at least 10-15ºC, to allow measurable heat exchange through the element. Humidity, rain and snow should be avoided 24-48 hours prior to the tests, since they can reduce the measured temperature values.

Tests should be carried out in areas of the wall without anomalies (i.e. moisture, thermal bridges and cold spots, among others). For this reason and before the on-site test, a qualitative infrared thermography inspection must be performed. It should be pointed out that the influence of the weather (wind, sun, rain, sky conditions, etc) may last for 2-6 hours, depending on the façades.

Some additional test conditions were determined from the developed research. Tests should avoid a non-stationary regime as well as a non-homogeneity of heat flux and temperature on the material. Consequently, special attention must be paid to the type of building façade, the external conditions or the internal climatic conditions (i.e. type of heating system). Firstly, heated adjacent walls may influence the thermal behaviour of the sample that is being tested, especially in single-leaf building façades. Wall temperature in the corners tends to be higher than the rest of the wall and, consequently, U-value uncertainty may be increased. Secondly, outdoor air temperatures remain more constant during some periods of the day. The tests should be undertaken at the start of the day, to ensure an optimum temperature difference (ΔT) without peaks. Thirdly, any air current peak generated when the inner air temperature is under the set point temperature may lead to a fluctuation in internal parameters.

POSTPRINT

2.2. Selection of the measuring equipment

An IR camera, a reflector and a blackbody are needed to measure quantitatively on-site U-values by means of IRT. Thermocouples with a data logger, or a thermohygrometer, are required to measure environmental conditions.

Several researchers have specified in their studies that the minimum requirements for an IR camera are related to: the spectral range, the spatial resolution, the temperature range, the thermal sensitivity, the frame rate and the angle of tilt. Taking into account that bodies at ambient temperature emit predominantly at 7-13 μm (spectral range), the IR camera should be selected for long wave length band [60, 61, 26, 40, 18, 41, 62, 49, 63, 50, 52]. The spatial resolution, also known as the Instantaneous Field of View (IFOV), is the ability of the camera to distinguish between two objects within the field of view (FOV). In other words, it is the smallest detail within the FOV that can be detected or seen at a set distance. Along this line, Bagavathiappan et al. [41] and Fox et al. [63] stated that FOV depends on the object to camera distance, the lens systems and the detector size. Its value represented in mrad corresponds to the size of the visible point in

millimetres of a pixel at a distance of 1 metre. For building diagnosis, FOV is described in horizontal degrees by vertical degrees, 25º x 19º, and IFOV is established as 1.36 mrad. Furthermore, Bagavathiappan et al. [41] mentioned that the temperature range is the minimum and maximum temperature values, typically -20ºC to 500ºC-; the thermal sensitivity should be selected as 0.05ºC for uncooled cameras and 0.01ºC for cooled cameras; and the number of frames acquired by the IR camera per second (frame rate) is normally set at 50Hz. Finally and as shown in Figure 2, to avoid any reflection of the thermographer in the resulting images, the angle of tilt should be a minimum of 5º from the thermographer to the target object to a maximum of 50º –from the horizontal- [63, 52].

Before making the measurements, the IR camera should be calibrated for the wall. In other words, the reflected ambient temperature (T_{REF}) as well as the wall surface emissivity are required to compensate errors of reading with the IR camera. These parameters allow reliable surface temperature values to be obtained in the area of known emissivity during the post–processing of each thermogram [5, 26, 62, 64, 25, 21].

The average reading of T_{REF} represents the average temperature of the surroundings, considering the different reflection indexes. To determine this parameter, a crinkled piece of aluminium foil fixed on the surface should be used as a reflector or substitute for Lambert's radiator [26, 40, 27, 62, 17, 64, 21, 58, 28]. In order to avoid uncontrolled reflection indexes, the wall under measurement needs to be free of any object [26]. A blackbody is needed to measure the wall surface emissivity. In thermal radiation theory, a blackbody is considered a hypothetical object that absorbs all incident radiation and radiates a continuous spectrum, according to Planck's Law and the Stefan-Boltzmann Law [60, 61, 26, 41, 64, 21]. The blackbody can be black tape, curved plastic hosepipe (with a hole 1cm^2 wide) or a blackbody simulator fixed to the target. A smoked metallic sheet cannot be used as a blackbody, because it does not achieve the target surface temperature.

Finally, some uncertainties may arise in the measuring chain due to the temperature sensor and its data logger. For this reason, the type of sensor (thermocouple type K or thermistor), the position of the sensor, sensor linearity and the sensitivity, sensor drift and calibration of the element should be taken into account. Type K thermocouples with a resolution of 0.1ºC and an accuracy of ± 0.4% + 1ºC are preferred. The data logger must enable measurements within the temperature range 0 to 50ºC, and a relative humidity below 85%. In addition, the data acquisition interval should be 1 second to 3600 seconds.

POSTPRINT

2.3. Data acquisition and post-processing

The IR camera should be positioned on a tripod perpendicular to the wall at a distance of 1.5 metres and an angle of 15º, to avoid its own reflection on the building element. This distance is enough to analyse a wide wall area characteristic of the thermal behaviour of the building façade, including the reflector foil.

Measurements should be performed and recorded over a period of 2-3 hours, with a data acquisition interval of 1 minute by the IR camera and FLIR TOOLS+ software [65]. Therefore, each test involves the analysis of a sequential video with 121 to 181 thermograms. All data loggers are configured to collect measurements from temperature sensors with the same data acquisition interval as the IR camera (1 minute). Surrounding environmental conditions are also continuously monitored and recorded during the on-site test duration by data loggers and thermocouples.

Post-processing of thermograms is carried out with the software mentioned above. The instantaneous readings of the wall surface temperature (T_{WALL}) and the reflected ambient temperature (T_{REF}) of each thermogram must be considered to determine the measured U-value. The average reflected ambient temperature (T_{REF}) should be measured in an area of the reflector located at 1.5 m above ground level to avoid any reflection of the ground and most of the furniture. In addition, the thermocouple of T_{IN} should be positioned at the same height. As this IRT method is performed inside the building, the height of the walls is around 2.5-3.0 m. Hence, a height of 1.5 m is acceptable to consider an average inner air temperature value, approximately equal to T_{REF}. The wall surface temperature (TWALL) should be calculated by measuring the maximum, minimum and average values of the total area of the building element that is being evaluated (Figure 2).

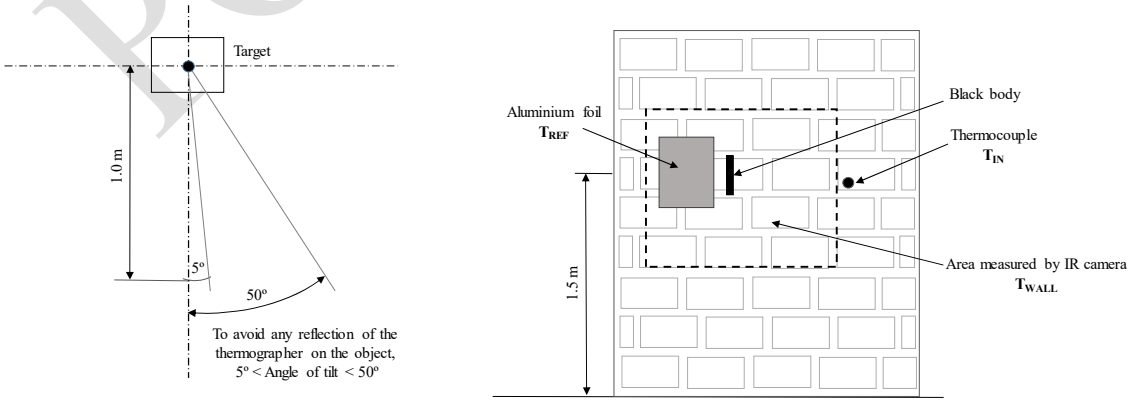

Figure 2. Top and front view of the position of the measuring equipment in relation to the wall

POSTPRINT

2.4. Calculation of the instantaneous measured U-value using the numerical model

Along the lines of the quantitative IRT, the proposed method determines the total thermal transmittance of a wall from inside the building envelope. According to Equation 1, the radiation interchange (qr) between the inner wall surface and its surroundings must be measured. In the same way, the convection heat transfer (qc) at the surface element must be calculated, without the influence of any kind of external stimulus (such as solar radiation, lamps, ovens etc).

$$U_{mes}\left[\frac{W}{m^2 \cdot K}\right] = \frac{q}{(T_{IN} - T_{OUT})} = \frac{(q_r + q_c)}{(T_{IN} - T_{OUT})} \quad (1)$$

Where U_{mes} denotes the measured U-value [W/ (m^2·K)]; q [W/m^2] is the specific heat flux through the building envelope including the specific heat flux by radiation q_r [W/m^2] and the specific heat flux by convection q_c [W/m^2]; T_{IN} is the air temperature near the target from inside the building [K]; T_{OUT} is the outdoor air temperature near the target [K]; and $T_{IN} - T_{OUT}$ is the temperature difference between inside and outside the building [K]. Each term of Equation 1 is explained below.

Radiation heat transfer (q_r)

Heat transfer through radiation takes place in the form of electromagnetic waves, mainly in the infrared region. The radiation energy per unit of time from a blackbody can be expressed with the Stefan-Boltzmann Law. During the cold season, the surroundings radiate energy to a cooler object, such as an inner wall surface, which leads to a net radiation heat loss rate (Equation 2) that can be defined as:

$$q_r\left[\frac{W}{m^2}\right] = \varepsilon_{WALL} \cdot \sigma \cdot \left[{T_{REF}}^4 - {T_{WALL}}^4\right] \quad (2)$$

Where q_r represents the specific heat flux by radiation [W/m^2]; ε_{WALL} is the emissivity coefficient of the object ($0 < \varepsilon < 1$, depending on the type of material and the temperature of the surface); σ is Stefan–Boltzmann's constant with a value of 5.67×10^{-8} [W/m^2 ·K^4]; A represents the area of the target [m^2]; T_{REF} denotes the reflected ambient temperature [K]; and T_{WALL} is the wall surface temperature from inside the building [K].

Convective heat transfer (q_c)

The heat energy transferred between a surface and a moving fluid at different temperatures is known as convection. Considering natural convection and laminar flow, the heat transfer per unit surface through convection (Equation 3) is known as Newton's Law of Cooling. In the same way as in heat transfer by radiation, the

POSTPRINT

cooler object is the wall to be tested. The equation for convection can be expressed as:

$$q_c \left[\frac{\mathrm{W}}{m^2}\right] = h_c \cdot [T_{IN} - T_{WALL}] \quad (3)$$

Where q_c belongs to specific heat flux by convection [W/m^2]; h_c is the convective heat transfer coefficient [W/m^2 ·K]; T_{IN} denotes the air temperature near the target from inside the building [K] and T_{WALL} is the wall surface temperature from inside the building [K].

According to Dall'O et al. [27], the external convective heat transfer coefficient tabulated in UNE-EN ISO 6946:2012 [35] is a high and precautionary value, since it is used to determine the heat loss during the design stage of the building façade. Therefore, the same assumption could be made in relation to the ISO value for the internal convective heat transfer coefficient. For this reason, in this developed method, the convective heat transfer coefficient is calculated with the dimensionless approach, as it is more accurate [32]. To determine the convective heat transfer coefficient, the Nusselt number (Equation 4) can be calculated as follows:

$$N_U = (h_c \cdot L)/k \quad (4)$$

As mentioned above, h_c is the convective heat transfer coefficient [W/m^2 ·K]. *Nu* is the Nusselt number [dimensionless] and *L* refers to the height of the wall [m] seen from inside the building. *k* is the thermal conductivity of the fluid. Taking into account that the fluid is air, *k* is equal to 0.025 W/m·K for a temperature between 20 and 25ºC. Even so, when the surface consists of a vertical plate such as a wall, the expression that describes the Nusselt number is the following (Equation 5).

$$N_U = \left\{0.825 + \frac{0.387 \cdot {R_a}^{1/6}}{\left[1+\left(\frac{0.492}{P_r}\right)^{9/16}\right]^{8/27}}\right\}^2 \quad (5)$$

Where R_a and P_r are the Rayleigh and Prandtl numbers respectively. The Prandtl number for air is considered to be 0.73 for an air temperature between 20 and 25ºC. The Rayleigh number (Equation 7), which is the product of Grashof (Equation 6) and Prandtl numbers, should be 10^4 <Ra <10^{10} for a laminar flow. It should be noted that all of these parameters are dimensionless.

POSTPRINT

$$G_r = \frac{g \cdot \beta \cdot (T_{IN} - T_{WALL}) \cdot L^3}{v^2} \quad (6)$$

$$R_a = G_r \cdot P_r = \frac{g \cdot \beta \cdot (T_{IN} - T_{WALL}) \cdot L^3}{v^2} \cdot P_r \quad (7)$$

The g refers to gravitation (9.8 m/s^2). The β is the volumetric temperature expansion coefficient [1/K], where all fluid properties should be evaluated at the film temperatures, so $\beta=1/T_m$ where $T_m= (T_{IN}+T_{WALL})/2$. The v is the air viscosity with a value of $1.5 \cdot 10^{-5}$ m^2/s for an air temperature between 20ºC and 25ºC. Replacing by the known values, the Rayleigh number (Ra) can be expressed as a function (Equation 8) that depends on the inner air temperature [K], the inner wall surface temperature [K] and the height of the wall [m]:

$$R_a = 3.18 \cdot 10^{10} \cdot \beta \cdot (T_{IN} - T_{WALL}) \cdot L^3 \quad (8)$$

From (4) and (5), the convective heat transfer coefficient becomes:

$$h_c \left[\frac{\mathrm{W}}{m^2 \cdot \mathrm{K}}\right] = \frac{\left\{0.825 + \frac{0.387 \cdot R_a^{\frac{1}{6}}}{\left[1+\left(\frac{0.492}{Pr}\right)^{\frac{9}{16}}\right]^{\frac{8}{27}}}\right\}^2 \cdot k}{L} \quad (9)$$

Taking into account the value of the Prandtl number, Equation 9 can be simplified.

$$h_c \left[\frac{W}{m^2 \cdot K}\right] = (k/L) \cdot \left\{0.825 + 0.325 \cdot R_a^{\frac{1}{6}}\right\}^2 \quad (10)$$

Determination of the instantaneous measured U-value

The instantaneous measured U-value [W/ (m^2·K)] for the winter season is denoted as Umes i and can be calculated by Equation 11 or its simplified version (Equation 12):

$$U_{mes_i} \left[\frac{W}{m^2 \cdot K}\right] = \frac{\left\{0.825 + \frac{0.387 \cdot R_a^{\frac{1}{6}}}{\left[1+\left(\frac{0.492}{Pr}\right)^{\frac{9}{16}}\right]^{\frac{8}{27}}}\right\}^2 \cdot k}{L} \cdot [T_{IN} - T_{WALL}] + \varepsilon \cdot \sigma \cdot \left[{T_{REF}}^4 - {T_{WALL}}^4\right]}{(T_{IN} - T_{OUT})} \quad (11)$$

POSTPRINT

$$U_{mes_i}\left[\frac{W}{m^2\cdot K}\right]=\frac{(k/L)\cdot\left\{0.825+0.325\cdot R_a^{\frac{1}{6}}\right\}^2\cdot[T_{IN}-T_{WALL}]+\varepsilon\cdot\sigma\cdot[{T_{REF}}^4-{T_{WALL}}^4]}{(T_{IN}-T_{OUT})} \quad (12)$$

2.5. Determination of the average measured U-value using the numerical model

According to ISO 9869-1:2014 [20] and taking into account all instantaneous measured U-values ($U_{mes\ i}$) through Equation 11, the average measured U-value (Umes avg) can be calculated using the average method (Equation 13).

$$U_{me\ avg}\left[\frac{W}{m^2\cdot K}\right]=\frac{\sum_{i=1}^{n}(q_{r_i}+q_{c_i})}{\sum_{i=1}^{n}(T_{IN_i}-T_{OUT_i})}=\frac{U_{mes_i}}{n} \quad (13)$$

Where *n* denotes the total number of thermograms that have been analysed.

3. VALIDATION OF THE METHOD

As shown in Figure 3, the validation of the method was focused on evaluating the accuracy of the measurement by means of comparison with the notional U-value (U_t). Furthermore, for each building investigated, the authors also determined the measured thermal transmittance using tabulated values from international standards, in order to check their influence on the measured U-value in comparison with the method.

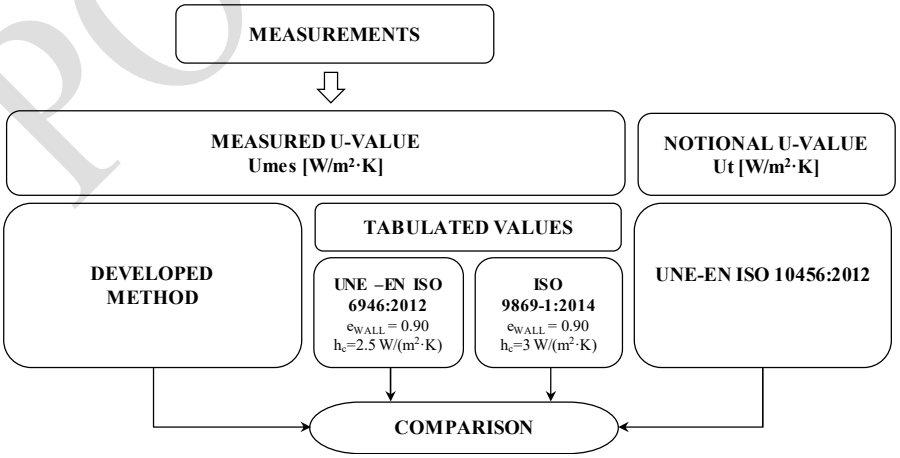

Figure 3. Flowchart of the validation process through case studies

POSTPRINT

The first standard, UNE-EN ISO 6946:2012 [35], establishes a wall surface emissivity of 0.90 and a convective heat transfer coefficient of h_c=2.5 W/m^2·K. The second standard, ISO 9869-1:2014 [20], notes the same emissivity but h_c=3 W/m^2·K. Hence, considering the instantaneous readings of T_{WALL} and T_{REF} obtained by IRT as well as the readings of the thermocouples in each test, three average measured U-values were calculated, one of them by the proposed model and the others through the tabulated values.

Regarding the comparison with the notional U-value, Ficco et al. [6] established that the estimation of the notional U-value of existing buildings can be based on four approaches: (1) using data obtained by historical analysis of the building or analogies with similar buildings using specific technical databases; (2) using nominal design data; (3) the actual data obtained by structure identification (sampling or endoscope method); (4) in-situ measurement using HFM.

In this research, the theoretical thermal transmittance of the building façade was estimated for each case study through the nominal design data following the technical data available in the Spanish Technical Building Code [66] and European Standards such as UNE-EN ISO 10456:2012 [73] and UNE-EN ISO 6946:2012 [35]. In particular, UNE-EN ISO 10456:2012 [73] provides the thermal properties for each building material, including thermal conductivity and resistance values in function of the material density or for an interval of densities, to estimate design values [26, 6, 67]. The theoretical thermal transmittance (U_t) for building façades can be calculated as follows (Equation 14):

$$U_t \left[\frac{W}{m^2 \cdot K}\right] = \frac{1}{R_t} = \frac{1}{R_{Si} + \sum_{i=0}^{n} \frac{\Delta x}{\lambda} + R_{Se}} = \frac{1}{0.13 + \sum_{i=0}^{n} \frac{\Delta x}{\lambda} + 0.04} \quad (14)$$

Where R_t is the theoretical thermal resistance [(m^2·K)/W]; R_{si} and R_{se} denote the theoretical thermal resistance from inside and outside the building [(m^2·K)/W] respectively; Δx is the thickness of the sample in metres; and λ is the thermal conductivity of the sample [W/(m·K)].

Therefore, the deviation between notional and measured U-value is expressed by (15) and (16):

$$\Delta U[W/(m^2 \cdot K)] = U_{mes_{avg}} - U_t \quad (15)$$

$$\Delta U/U_t\ [\%] = (U_{mes_{avg}} - U_t)/U_t \quad (16)$$

POSTPRINT

To determine the combined standard uncertainty based on all the measured parameters from Equation 11, ISO/IEC Guide 98-3:2008 (International Organization for Standardization, 2008) was taken into account as well as the accuracy of the measuring equipment (sensors and infrared camera). The uncertainity (σU) for the proposed method was obtained using the following expression:

$$(\sigma U_{mes})^2 = \left(\frac{\delta U_{mes}}{\delta T_{IN}}\right)^2 \cdot (\sigma T_{IN})^2 + \left(\frac{\delta U_{mes}}{\delta T_{OUT}}\right)^2 \cdot (\sigma T_{OUT})^2 + \left(\frac{\delta U_{mes}}{\delta T_{WALL}}\right)^2 \cdot (\sigma T_{WALL})^2 + \left(\frac{\delta U_{mes}}{\delta T_{REF}}\right)^2 \cdot (\sigma T_{REF})^2 + \left(\frac{\delta U_{mes}}{\delta \varepsilon_{WALL}}\right)^2 \cdot (\sigma \varepsilon_{WALL})^2 \quad (17)$$

Where σT_{IN} and σT_{OUT} are the uncertainties associated with the environmental indoor and outdoor temperature measuring equipment respectively. σT_{WALL}, σT_{REF} and $\sigma \varepsilon_{WALL}$ are the uncertainties associated with the infrared camera when the wall surface temperature, the reflected ambient temperature and the wall emissivity are measured respectively.

Notably, some parameters of the numerical model (N_u –Nusselt number-, β -volumetric temperature expansion coefficient-, R_a –Rayleigh number- and h_c -convective heat transfer coefficient-) in relation to convective heat transfer (q_c) are a function of T_{IN} and T_{WALL}. When tabulated values are used, the procedure should be the same, but it should be considered that h_c is no longer a function of T_{IN} and T_{WALL} to be derived from Equation 11.

4. CASE STUDIES

According to Gangolells et al., [69], 59% of the current Spanish residential building stock was erected before the first thermal regulation NBE-CT-79 [70]. Nearly 38% of Spanish residential buildings already in use were built under NBE-CT-79 [70], satisfying the minimum thermal requirements. Three per cent of Spanish residential building stock was erected under Spanish Technical Building Code CTE-DB-HE1 [66]. Along this line, Gangolells et al. [71] stated that 53.6% of residential buildings with energy certification had the worst energy label (E class). For these reasons, two typical Spanish wall typologies from different periods were chosen as case studies.

Case study A is a single–leaf wall that is 3.26 metres high, corresponding to the typical building façade erected before NBE-CT-79 [70]. Case study B is a sample that is 2.54 metres high and consists of a multi-leaf wall (external insulation), built under CTE-DB-HE1 [66]. The main technical features and thermo-physical properties of these building façades and a sketch of them are shown in Tables 1 and 2 respectively. In accordance with the method explained above, the

POSTPRINT

measurement campaign took place during January and February 2016, to ensure a temperature difference across the building façade that was within 10-15ºC.

Table 1. Technical characteristics and thermo-physical properties of case study A (from outside to inside)

#	Case Study A	Δx [m]	c [J/Kg·K]	ρ [Kg/m^3]	λ [W/(m·K)]	R-value [(m^2·K)/W]	Sketch
1	Mortar	0.02	1000	1900	1.30	---	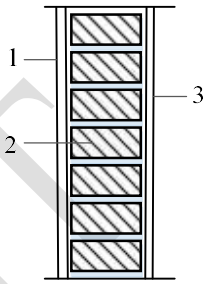
2	Perforated brick	0.14	1000	920	---	0.23	
3	Internal plaster	0.01	1000	1000-1300	0.57	---	
R_{se} = 0.04 (m^2·K)/W							
R_{si} = 0.13 (m^2·K)/W							
U_t = 2.31 W/(m^2·K)							

Δx: thickness; c: thermal capacity; ρ: density; λ: thermal conductivity; R-value: thermal resistance of the material; R_{se}: theoretical thermal resistance from outside the building; R_{si}: theoretical thermal resistance from inside the building; U_t: theoretical thermal transmittance.

Table 2. Technical characteristics and thermo-physical properties of case study B (from outside to inside)

	Case Study B	Δx [m]	c [J/Kg·K]	ρ [Kg/m^3]	λ [W/(m·K)]	R-value [(m^2·K)/W]	Sketch
1	Mortar	0.002	1000	1900	1.30	--	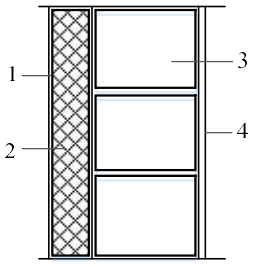
2	Insulation EPS	0.06	--	--	--	1.62	
3	Thermoclay	0.24	--	--	--	0.57	
4	Internal plaster	0.01	1000	1000-1300	0.57	--	
R_{se} = 0.04 (m^2·K)/W							
R_{si} = 0.13 (m^2·K)/W							
U_t = 0.42 W/(m^2·K)							

Δx: thickness; c: thermal capacity; ρ: density; λ: thermal conductivity; R-value: thermal resistance of the material; R_{se}: theoretical thermal resistance from outside the building; R_{si}: theoretical thermal resistance from inside the building; U_t: theoretical thermal transmittance.

POSTPRINT

First, qualitative inspections by IRT were conducted in both case studies. No anomalies were detected. These inspections helped in decision of which wall area should be analysed.

Considering northern façades for both case studies, six tests were performed under different measuring conditions. In case study A (single-leaf wall built before NBE-CT-79 [70]), two tests were carried out: test A.1. was developed without heating; test A.2. was executed with the heating system switched on 48 hours previously. In case study B (multi-leaf wall erected under CTE-DB-HE1 [66]), the building did not have a heating system. Typically, outside temperatures range from 0 to 5ºC between 6 am and 9 am during the winter. In addition, inner air temperature normally remains at 12 – 14ºC in unoccupied buildings. Therefore, a temperature difference within the range of 8 to 10ºC can be ensured between the inside and outside of the building.

In both case studies, the reflected ambient temperature (T_{REF}) was measured using crinkled aluminium foil. The reflector and the wall areas were monitored with a data acquisition interval of 1 minute. The wall surface emissivity (ε_{WALL}), determined by black tape, was found to be 0.88. The main technical characteristics of the measuring equipment are shown in Table 3.

Table 3. Main technical specifications of the equipment

Equipment	Input	Measuring range	Resolution	Accuracy
Infrared camera Model: FLIR E60bx	T_{WALL} T_{REF}	Temperature: -20ºC to +120ºC FOV: 25º x 19º; IFOV: 1.36 mrad Spectral Range: 7.5 - 13 µm Thermal sensitivity at 60 Hz: <0.045ºC at 30ºC / 45mK Sensor: FPA, uncooled microbolometer	320 x 240 pixels	±2ºC or ± 2% reading (ambient temperature 10ºC to 35ºC)
Data logger PCE-T390 with thermocouples K	T_{IN} T_{OUT}	Temperature -50.1ºC to 100ºC Humidity <85%	0.1ºC	±(0.4% + 0.5ºC)

5. DISCUSSION OF THE RESULTS

The results of the case studies are presented in Tables 4, 5 and 6. As mentioned in Section 3, the notional U-values were estimated by UNE-EN ISO 10456:2012 [73]. To check the influence of using tabulated values instead of the developed method to determine the thermal transmittance of walls, the deviations between the measured U-values obtained by quantitative IRT and UNE -EN -ISO 6946:2012 [35] as well as ISO 9869-1:2014 [20] were calculated respectively.

POSTPRINT

The comparative analysis of the measured U-values calculated using the proposed method and the notional U-values showed a deviation of 1.24% to 3.97%. Conversely, the deviation between the notional and the measured U-values was found to be 14 -28% for the HFM [20] or 10 -20% for other methods of quantitative IRT developed in recent years [5, 26, 52, 17, 64, 25]. Therefore, the proposed method has two advantages. Firstly, it can be used to achieve greater accuracy than other methods. Secondly, it requires less execution time. In fact, the test takes 2-3 hours in comparison to a minimum of 72 hours and maximum of one week for the HFM method.

A further comparative analysis was carried out to evaluate the influence of using tabulated values rather than the proposed method to determine measured U-values. For this in-depth analysis, the measured values of emissivity (ε_{WALL}) and convective heat transfer (h_c) were combined with the tabulated values of UNE-EN ISO 6946:2012 [35] and ISO 9869-1:2014 [20] to obtain different U-values and assess the role of these parameters. The options to be calculated were as follows:

a) U-value with the proposed method.
b) U-value maintaining the measured emissivity and using the tabulated value of hc from UNE EN-ISO 6946:2012 (ε_{WALL} = 0.88; h_c=2.5 W/m^2·K)
c) U-value maintaining the calculated hc and using the tabulated value of emissivity from UNE EN-ISO 6946:2012 (h_c from the method; ε_{WALL} = 0.90)
d) U-value with the tabulated values of emissivity and hc from UNE EN-ISO 6946:2012 (ε_{WALL} = 0.90; h_c=2.5 W/m^2·K)
e) U-value maintaining the emissivity and using the tabulated value of hc from ISO 9869-1:2014 (ε_{WALL} = 0.88; h_c=3 W/m^2·K)
f) U-value maintaining the calculated hc and using the tabulated value of emissivity from ISO 9869-1:2014 (h_c from the method; ε_{WALL} = 0.90)
g) U-value with the tabulated values of emissivity and hc from ISO 9869-1:2014 (ε_{WALL} = 0.90; h_c=3 W/m^2·K)

The c) and f) options produced the same result, since the tabulated value of the emissivity is equal. Notably, the value of hc is slightly different to that obtained in a), since another value of emissivity (ε_{WALL} =0.90) involves a new analysis for each thermogram of the test and consequently, new values of T_{WALL} in the numerical model.

For the single-leaf wall when the room was without heating (test A.1, Table 4), the proposed method had a deviation of 2.16% in comparison with 6.66% and 14.94% using tabulated values. In the same case study, when the room was heated for 48 hours prior to the test (test A.2, Table 5), the proposed method showed a deviation of 1.24% with respect to 3.06% and 13.28% using tabulated values.

POSTPRINT

Table 4. Case study A.1. Comparison between notional and measured U-value using quantitative IRT, UNE-EN ISO 6946:2012 and ISO 9869-1:2014 (absolute deviations are presented as a percentage)

Case study A.1. Without heating 8.7ºC < ΔT < 9.8ºC 181 thermograms		**MEASURED U-VALUE Umes [W/m²·K]**			**NOTIONAL U-VALUE Ut [W/m²·K]**
		DEVELOPED METHOD	**UNE-EN ISO 6946:2012**	**ISO 9869-1:2014**	**UNE-EN ISO 10456:2012**
DEVELOPED METHOD	**ε = 0.88**	**h_c = 2.142 W/m²·K** 2.360 ± 0.280 (2.16%)	**h_c = 2.5 W/m²·K** 2.449 ± 0.278 (8.18%)	**h_c = 3 W/m²·K** 2.695 ± 0.293 (16.67%)	2.310
UNE –EN ISO 6946:2012 ISO 9869-1:2014	**ε = 0.90**	**h_c = 2.125 W/m²·K** 2.322 ± 0.282 (0.51%)	**h_c = 2.5 W/m²·K** 2.464 ± 0.280 (6.66%)	**h_c = 3 W/m²·K** 2.655 ± 0.295 (14.94%)	

U_{mes}: measured thermal transmittance; U_t: notional thermal transmittance; $\Delta T = T_{IN}-T_{OUT}$; ε_{WALL}: emissivity of the wall; h_c: convective heat transfer coefficient.

Table 5. Case study A.2. Comparison between notional and measured U-value using quantitative IRT, UNE-EN ISO 6946:2012 and ISO 9869-1:2014 (absolute deviations are presented as a percentage)

Case study A.2. With heating (>48h previously) 7ºC < ΔT < 15.8ºC 181 thermograms		**MEASURED U-VALUE U_{mes} [W/m²·K]**			**NOTIONAL U-VALUE U_t [W/m²·K]**
		DEVELOPED METHOD	**UNE-EN ISO 6946:2012**	**ISO 9869-1:2014**	**UNE-EN ISO 10456:2012**
DEVELOPED METHOD	**ε_{WALL} = 0.88**	**h_c = 2.370 W/m²·K** 2.339 ± 0.335 (1.24%)	**h_c = 2.5 W/m²·K** 2.395 ± 0.320 (3.71%)	**h_c = 3 W/m²·K** 2.634 ± 0.337 (14.05%)	2.310
UNE –EN ISO 6946:2012 ISO 9869-1:2014	**ε_{WALL} = 0.90**	**h_c = 2.361 W/m²·K** 2.320 ± 0.340 (0.44%)	**h_c = 2.5 W/m²·K** 2.380 ± 0.324 (3.06%)	**h_c = 3 W/m²·K** 2.617 ± 0.341 (13.28%)	

U_{mes}: measured thermal transmittance; U_t: notional thermal transmittance; $\Delta T = T_{IN}-T_{OUT}$; ε_{WALL} : emissivity of the wall; h_c: convective heat transfer coefficient.

For the multi-leaf wall (external insulated building façade), the results were even more relevant. Considering the results of Table 6 for test B, the proposed method had a deviation of 3.97% compared to 30.15% and 42.87% according to the two regulations mentioned above.

POSTPRINT

Table 6. Case study B. Comparison between notional and measured U-value using quantitative IRT, UNE-EN ISO 6946:2012 and ISO 9869-1:2014 (absolute deviations are presented as a percentage)

Case study B **Without heating** **8.7ºC < ΔT < 9.8ºC** **121 thermograms**		**MEASURED U-VALUE** U_{mes} **[W/m²·K]**			**NOTIONAL U-VALUE** U_t **[W/m²·K]**
		DEVELOPED METHOD	**UNE-EN ISO 6946:2012**	**ISO 9869-1:2014**	**UNE-EN ISO 10456:2012**
DEVELOPED METHOD	ε_{WALL} **= 0.88**	h_c **= 1.456 W/m²·K** 0.437 ± 0.219 (3.97%)	h_c **= 2.5 W/m²·K** 0.548 ± 0.243 (30.47%)	h_c **= 3 W/m²·K** 0.602 ± 0.266 (43.32%)	0.420
UNE –EN ISO 6946:2012 **ISO 9869-1:2014**	ε_{WALL} **= 0.90**	h_c **= 1.451 W/m²·K** 0.436 ± 0.222 (3.80%)	h_c **= 2.5 W/m²·K** 0.547 ± 0.246 (30.15%)	h_c **= 3 W/m²·K** 0.601 ± 0.269 (42.87%)	

U_{mes}: measured thermal transmittance; U_t: notional thermal transmittance; $\Delta T = T_{IN}-T_{OUT}$; ε_{WALL} : emissivity of the wall; h_c: convective heat transfer coefficient.

As seen, the measurements were only slightly influenced by the wall surface emissivity (ε_{WALL}). In contrast, overestimated tabulated values for the convective heat transfer coefficient lead to high deviations in U-value. Considering the results of Tables 4 and 5 for case study A, the discrepancy between the measured and the tabulated values of hc was low: 2.142 W/m²·K without heating or 2.370 W/m²·K. with heating, compared to 2.5 and 3 W/m²·K. In accordance with Table 6, the measured hc showed a value of 1.456 W/m²·K in comparison with the tabulated values of 2.5 and 3 W/m²·K. Consequently, tabulated values for the convective heat transfer coefficient (h_c) might not be suitable for heavy walls with low U-values.

In the literature, quantitative IRT tests were conducted under a temperature difference range between 10ºC and 15ºC. Using the method reported in this paper, the value can be reduced to the lowest level of the temperature difference range (7º < ΔT < 16ºC), achieving a high level of accuracy. Therefore, the proposed method can be used to measure U-values in unoccupied buildings without heating systems.

The period of time that the internal heating system had been switched on prior to the test might not have had any influence on good heat flux transfer from inside to outside the building façade (Tables 4, 5 and 6). By way of example, Figure 4 shows the main measured parameters over time as well as the measured U-value by quantitative IRT with its corresponding uncertainty. At the beginning of the test, the instantaneous U-values were slightly lower than the theoretical U-value. During the test, T_{REF} and T_{WALL} remained around the initial value, with minimum fluctuations.

POSTPRINT

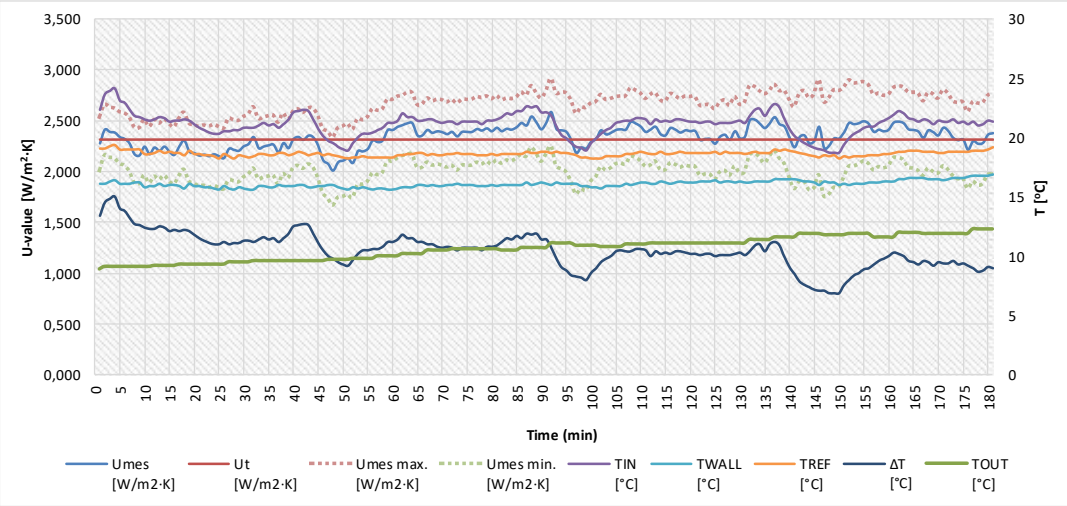

Figure 4. Measured parameters over time in case study A.2

As stated above, when the test was performed without a heating system, the deviation was found to be reliable. For existing buildings that had not been used for a long-term (case study A) or buildings recently built without connection to the electrical grid and heating system (case study B), it was not important to maintain steady-state conditions 48 hours before the measurements, because the boundary conditions had not been altered previously.

As stated by Danielski and Fröling [21], the large wall areas had lower temperature uniformity (2-3ºC), which is considered the difference between the maximum and minimum inner wall surface temperature, in comparison with the small wall areas (<0.5ºC). In a single–leaf wall and as shown in Figure 5, the temperature uniformity and the discrepancies between the notional and measured U-value can be attributed to singular elements (i.e. the proportion of mortar compared to brick for the small areas; the influence of the corner where the temperatures are higher than the rest of the wall for large areas). In contrast, a multi-leaf wall can present a higher degree of uniformity, since any part of the element has the same average wall surface temperature (Figure 6). In order to quantify the influence of the analysed wall area of the thermogram on the determination of the U-value, several areas were defined. The optimum outcomes were given by an area of 104x221 (22984 pixels) for the single-leaf wall and an area of 146x212 (30952 pixels) for the multi-leaf wall. As an example of a non-homogeneus wall, the results for case study A.2. were shown in Table 7. It is concluded that the quantity of pixels is not as relevant as the homogeneity of heat flux and temperature on the material in the area that is being analysed.

POSTPRINT

Table 7. Case study A.2. Influence of the analysed wall area in the thermogram. Comparison between notional and measured U-value using quantitative IRT (absolute deviations are presented as a percentage).

AREAS	NUMBER OF PIXELS	MEASURED U-VALUE U_{mes} [W/m^2·K]	NOTIONAL U-VALUE U_t [W/m^2·K]
Ar3 (104 x 221)	22,984	2.339 ± 0.335 (1.24%)	2.310
Bx3 (226 x 63)	14,238	2.031 ± 0.334 (12.09%)	
EI1 (30 x 30)	900	2.575 ± 0.337 (11.49%)	
El2 (30 x 30)	900	2.299 ± 0.335 (0.49%)	

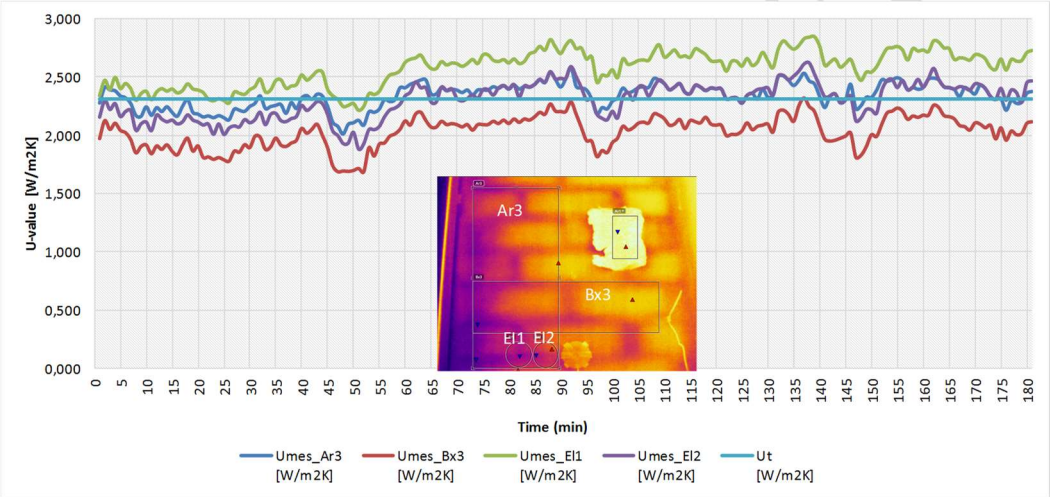

Figure 5. Case study A.2. Influence of the analysed wall area in the thermogram

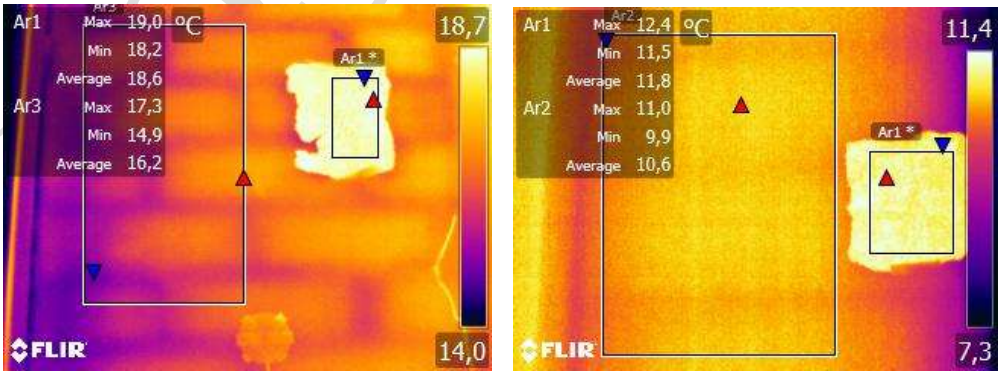

Figure 6. Wall surface temperature uniformity in case study A.2. (left) and case study B (right)

6. CONCLUSIONS

The main contribution of this research is the development of a new method to determine in-situ U-values using quantitative internal infrared thermography with a maximum deviation of 1.24 up to 3.97% and a test duration of 2 -3 hours. Moreover, this proposed method allows measurement from a temperature difference of 7 ºC, in contrast to the IRT methods carried out in recent years. In terms of execution time and data processing, this method was easier than the HFM method. Furthermore, measurements could be made with minimal instrumentation. In fact, the combination of qualitative and quantitative IRT in the same inspection allows an in-depth evaluation of the building envelope, instead of providing a local measurement.

The case studies demonstrated that the proposed method can be used in building façades under different measuring conditions, regardless of whether the construction is a single-leaf wall or a multi-leaf wall. In general, construction project documents for existing buildings, especially the oldest ones, are not available. Hence, this method may provide information about the building envelope for future refurbishment. In the case of new buildings, the method allows the thermal behaviour of building façades to be checked according to the design parameters. As seen above, this method represents a significant improvement on current regulations, especially for walls with low U-values (i.e. multi–leaf walls) where the use of tabulated values leads to overestimated thermal transmittances. Furthermore, this type of wall presents a higher degree of uniformity, which ensures homogeneity of the heat flux and temperature of the material, as well as minimum influence of the wall area that is being analysed in the thermogram during the post-processing stage to determine the measured U-value.

The new method does not require 48 hours as a test condition if the building has not been used recently, since the building is operating in steady-state conditions. This facilitates implementation of the method in buildings with heavy façades. In previous investigations carried out in recent years, new buildings were not evaluated and inner rooms of existing buildings needed to be at a uniform level of temperature for at least 48 hours.

Considering all of the aspects described above, it can be concluded that the proposed method may be of a great use to researchers and construction practitioners. As shown, the proposed method clearly improves all existing methods to determine the measured U-value in situ. In addition, construction practitioners and contractors can benefit from the application of the method to obtain reliable information on the performance of national building stock, to make decisions in relation to refurbishments, to reduce the energy performance gap in new buildings, among other aspects.

Finally, the proposed method could be a first step towards the proposal of a standard for assessing in-situ U-values in building façades by quantitative infrared thermography. Future steps of this research may include assessing the limits of the

POSTPRINT

temperature difference inside and outside the building as well as the shooting frequency of thermograms for reliable measured U-value results. In addition, it would be interesting to validate the method for light walls, which have less thermal mass and the impact of wind speed may be greater.

7. REFERENCES

[1] IEA -International Energy Agency-. Promoting Energy Efficiency Investments. Case Studies in the residential sector, 2008. Available at: <http://www.iea.org/publications/freepublications/publication/promotingee2008.pdf > (Accessed 04 October 2016)

[2] UNEP –United Nations Environment Programme-. Buildings and Climate Change. Summary for Decision Makers, 2009. Available at: <http://www.unep.org/sbci/pdfs/SBCI-BCCSummary.pdf > (Accessed 04 October 2016)

[3] BPIE -Buildings Performance Institute Europe-. Europe's Buildings Under The Microscope. A country-by-country review of the energy performance of buildings, 2011. Available at:<http://bpie.eu/wp-content/uploads/2015/10/HR_EU_B_under_microscope_study.pdf> (Accessed 04 October 2016)

[4] European Union, 2010. Directive 2010/31/EU of the European Parliament and of the Council of 19 May 2010 on the energy performance of buildings. Available at: <http://eur-lex.europa.eu/legal-content/EN/TXT/PDF/?uri=CELEX:32010L0031&from=en> (Accessed 04 October 2016)

[5] R. Albatici, A.M. Tonelli, Infrared thermos vision technique for the assessment of thermal transmittance value of opaque building elements on site. Energy Build. 42 (2010) 2177–2183.

[6] G. Ficco, F. Iannetta, E. Ianniello, F.R. d'Ambrosio, M. Dell'Isola. U-Value in situ measurement for energy diagnosis of existing buildings. Energy Build. 104(2013) 108–121.

[7] European Union, Directive 2012/27/EU of the European Parliament and of the Council of 25 October 2012 on Energy Efficiency, Amending Directive2009/125/EC and 2010/30/EU and Replacing Directives 2004/8/EC and2006/32/EC, 2012. Available at: http://eur-lex.europa.eu/legal-content/EN/TXT/PDF/?uri=CELEX:32012L0027&from=en (Accessed 04 October 2016).

POSTPRINT

[8] B. Bordass, R. Cohen, J. Field. Energy performance of non-domestic buildings: closing the credibility gap. International Conference on Improving Energy Efficiency in Commercial Buildings (2004).

[9] C. Demanuele, T. Tweddell, M. Davies. Bridging the gap between predicted and actual energy performance in schools. World Renewable Energy Congress XI, Abu Dhabi, UAE, 2010.

[10] A.C. Menezes, A. Cripps, D. Bouchlaghem, R. Buswell. Predicted vs. actual energy performance of non-domestic buildings: using post-occupancy evaluation data to reduce the performance gap. Appl. Energy 97 (2012)355–364.

[11] B. Dimitrijevic, J. Bros Williamson, C. Purdie, G. Morrison, The Gap Between Design and Build: Construction Compliance Towards 2020 in Scotland (2012). (CIC START ONLINE).

[12] O. Guerra -Santín, C. Tweed, H. Jenkins, S. Jiang, Monitoring the performance of low energy dwellings: two UK case studies. Energy Build. 64 (2013) 32–40.

[13] P. De Wilde. The gap between predicted and measured energy performance of buildings: a framework for investigation. Autom. Constr. 41 (2014) 40–49.

[14] M. Dowson, A. Poole, D. Harrison, G. Susman. Domestic UK retrofit challenge: barriers, incentives and current performance leading into the Green Dale. Energy Policy 50 (2012) 294–305.

[15] A. Zalejska-Jonsson. Evaluation of low-energy and conventional residential buildings from occupants' perspective. Build. Environ. 58 (2012) 135–144.

[16] S. Ferrari, V. Zanotto. The thermal performance of walls under actual service conditions: evaluating the results of climatic chamber tests. Constr. Build. Mater. 43 (2013) 309–316.

[17] I. Nardi, S. Sfarra, D. Ambrosini. Quantitative thermography for the estimation of the U-value: state of art and a case study. 32nd IUT (Italian Union of Thermo-Fluid-Dynamics) Heat Transfer Conference Journal of Physics, Conference Series 547 (2014) 012-016.

POSTPRINT

[18] R. Albatici, F. Passerini, A.M. Tonelli, S. Gialanella. Assessment of the thermal emissivity value of building materials using an infrared thermos vision technique emissometer. Energy Build. 66 (2013) 33–40.

[19] K. Gaspar, M. Casals, M. Gangolells. A comparison of standardized calculation methods for in situ measurements of façades U-value. Energy Build. 130(2016) 592–599.

[20] International Organization for Standardization, ISO 9869:2014 thermal insulation. Building elements, in: In-Situ Measurement of Thermal Resistance and Thermal Transmittance. Part 1: Heat Flow Meter Method, 2014.

[21] I. Danielski, M. Fröling, Diagnosis of buildings' thermal performance—a quantitative method using thermography under non-steady state heat flow. 7th International Conference on Sustainability in Energy and Buildings (2015)320–329. Energy Procedia.

[22] Infrared Training Center and FLIR Systems, 2015. Level I Infrared Thermography Certification Manual. Publication Number 1560093 G-es-ES. Spain, 2016.

[23] International Organization for Standardization, EN 13187:1998 (ISO6781:1983 Modified). Thermal Performance of Buildings. Qualitative Detection of Thermal Irregularities in Building Envelopes. Infrared Method,1998.

[24] RESNET-Residential Energy Services Network, RESNET Interim Guideline for Thermographic Inspections of Buildings, 2010, Available at: http://www.resnet.us/standards/RESNET_IR_interim_guidelines.pdf (Accessed 04 October 2016).

[25] R. Albatici, A.M. Tonelli, M. Chiogna. A comprehensive experimental approach for the validation of quantitative infrared thermography in the evaluation of building thermal transmittance. Appl. Energy 141 (2015) 218–228.

[26] P.A. Fokaides, S.A. Kalogirou. Application of infrared thermography for the determination of the overall heat transfer coefficient (U-value) in building envelopes. Appl. Energy 88 (2011) 4358–4365.

POSTPRINT

[27] G. Dall'O, L. Sarto, A. Panza. Infrared screening of residential buildings for energy audit purposes: results of a field test. Energies 6 (2013) 3859–3878.

[28] I. Nardi, D. Paoletti, D. Ambrosini, T. de Rubeis, S. Sfarra. U-value assessment by infrared thermography: a comparison of different calculation methods in a Guarded Hot Box. Energy Build. 122 (2016) 211–221.

[29] J.A. Palyvos. A survey of wind convection coefficient correlations for building envelope energy systems' modelling. Appl. Therm. Eng. 28 (2008) 801–808.

[30] A. Hoyano, K. Asano, T. Kanamaru. Analysis of the heat flux from the exterior surface of buildings using time sequential thermography. Atmos. Environ. 33(1999) 3941–3951.

[31] A.V. Rabadiya, R. Kirar. Comparative analysis of wind loss coefficient (wind heat transfer coefficient) for solar plate collector, Int. J. Emerg. Technol. Adv.Eng. (IJETAE) 2 (9) (2012) (ISSN 2250-2459).

[32] J.F.C. Sham, T.Y. Lo, S.A. Memon. Verification and application of continuous surface temperature monitoring technique for investigation of nocturnal sensible heat release characteristics by building fabrics. Energy Build. 53(2012) 108–116.

[33] M.G. Emmel, M.O. Abadie, N. Mendes. New external convective heat transfer coefficient correlations for isolated low −rise buildings. Energy Build. 39(2007) 335–342.

[34] J. Liu, M. Heidarinejad, S. Gracik, J. Srebric. The impact of exterior surface convective heat transfer coefficients on the building energy consumption in urban neighbourhoods with different plan area densities. Energy Build. 86(2015) 449–463.

[35] International Organization for Standardization, UNE EN ISO 6946:2012 (ISO6946:2007). Building Components and Building Elements. Thermal Resistance and Thermal Transmittance. Calculation Method, 2012.

[36] E. Grinzato, V. Vavilov, T. Kauppinen. Quantitative infrared thermography inbuildings. Energy Build. 29 (1998) 1–9.

POSTPRINT

[37] S. Martin Oca˜na, I. Ca˜nas Guerrero, I. Gonzalez Requena. Thermographic survey of two rural buildings in Spain. Energy Build. 36 (2004) 515–523.

[38] D. Aelenei, F.M.A. Henriques. Analysis of the condensation risk on exteriorsurface of building envelopes. Energy Build. 40 (2008) 1866–1871.

[39] G. Desogus, S. Mura, R. Ricciu. Comparing different approaches to in situmeasurement of building components thermal resistance. Energy Build. 43(2011) 2613–2620.

[40] F. Asdrubali, G. Baldinelli, F. Bianchi. A quantitative methodology to evaluatethermal bridges in buildings. Appl. Energy 97 (2012) 365–373.

[41] S. Bagavathiappan, B.B. Lahiri, T. Saravanan, J. Philip, T. Jayakumar. Infrared thermography for condition monitoring—a review. Infrared Phys. Technol. 60(2013) 35–55.

[42] A. Byrne, G. Byrne, A. Davies, A.J. Robinson. Transient and quasi-steady thermal behaviour of a building envelope due to retroffited cavity wall and ceiling insulation. Energy Build. 61 (2013) 356–365.

[43] P.G. Cesaratto, M. De Carli. A measuring campaign of thermal conductance in situ and possible impacts on net energy demand in buildings. Energy Build.59 (2013) 29–36.

[44] A. Kumar, B.M. Suman. Experimental evaluation of insulation materials for walls and roofs and their impact on indoor thermal comfort under composite climate. Build. Environ. 59 (2013) 635–643.

[45] B. Lehman, K. Ghazi Wakili, Th. Frank, B. Vera Collado, Ch. Tanner, Ch. Effects of individual climatic parameters on the infrared thermography of buildings. Appl. Energy 110 (2013) 29–43.

[46] A. Ahmad, M. Maslehuddin, L.M. Al-Hadhrami,.In situ measurement of thermal transmittance and thermal resistance of hollow reinforced precast concrete walls. Energy Build. 84 (2014) 132–141.

POSTPRINT

[47] F. Asdrubali, F. D'Alessandro, G. Baldinelli, F. Bianchi. Evaluating in situ thermal transmittance of green buildings masonries—a case study. Case Stud. Constr. Mater. 1 (2014) 53–59.

[48] P. Biddulph, V. Gori, C.A. Elwell, C. Scott, C. Rye, R. Lowe, T. Oreszczyn. Inferring the thermal resistance and effective thermal mass of a wall using frequent temperature and heat flux measurements. Energy Build. 78 (2014) 10–16.

[49] F. Bisegna, D. Ambrosini, D. Paoletti, S. Sfarra, F. Gugliermetti. A qualitative method for combining thermal imprints to emerging weal points of ancientwall structures by passive infrared thermography—a case study. J. Cult. Herit.15 (2014) 199–202.

[50] S.S. De Freitas, V.P. de Freitas, E. Barreira. Detection of façade plaster detachments using infrared thermography—a non-destructive technique. Constr. Build. Mater. 70 (2014) 80–87.

[51] E. Latif, M. Anca Ciupala, D. Chitral Wijeyesekera. The comparative in situ hygrothermal performance of hemp and stone wool insulations in vapour open timber frame wall panels. Constr. Build. Mater. 73 (2014) 205–213.

[52] A. Kylili, P.A. Fokaides, P. Christou, S.A. Kalogirou. Infrared thermography (IRT) applications for building diagnostics: a review. Appl. Energy 134 (2014) 531–549.

[53] A.L. Pisello, V.L. Castaldo, J.E. Taylor, F. Cotana. Expanding inter-building effect modelling to examine primary energy for lighting. Energy Build. 76 (2014) 513–523.

[54] M. Rossi, V.M. Rocco. External walls design: the role of periodic termal transmittance and internal areal heat capacity. Energy Build. 68 (2014)732–740.

[55] F. Stazi, F. Tittarelli, G. Politi, C. Di Perna, P. Munafo. Assessment of the actual hygrothermal performance of glass mineral wool insulation applied 25 years ago in masonry cavity walls. Energy Build. 68 (2014) 292–304.

POSTPRINT

[56] T. Taylor, J. Counsell, S. Gill. Combining thermography and computer simulation to identify and assess insulation defects in the construction of building façades. Energy Build. 76 (2014) 130–142.

[57] E. Vereecken, S. Roels. A comparison of the hygric performance of interior insulation systems: a hot box-cold box experiment. Energy Build. 80 (2014)37–44.

[58] M. Fox, D. Coley, S. Goodhew, P. de Wilde. Time- lapse thermography for building defect detection. Energy Build. 92 (2015) 95–106.

[59] K. Maroy, K. Carbonez, M. Steeman, N. Van Den Bossche, Assessing the thermal performance of insulating glass units with infrared thermography: potential and limitations. Energy Build. 138 (2017) 175–192.

[60] T. Astarita, G. Cardone, G.M. Carlomagno, C. Meola. A survey on infrared thermography for convective heat transfer measurements. Opt. Laser Technol.32 (2000) 593–610.

[61] N.P. Avdelidis, A. Moropoulou. Emissivity considerations in building thermography. Energy Build. 35 (2003) 663–667.

[62] C. Porras-Amores, F.R. Mazarron, I. Cañas. Using quantitative infrared thermography to determine indoor air temperature. Energy Build. 65 (2013)292–298.

[63] M. Fox, D. Coley, S. Goodhew, P. de Wilde. Thermography methodologies for detecting energy related building defects. Renew. Sustain. Energy Rev. 40(2014) 296–310.

[64] K.E.A. Ohlsson, T. Olofsson. Quantitative infrared thermography imaging of the density of heat flow rate through a building element surface. Appl. Energy134 (2014) 499–505.

[65] FLIR Systems, 2015. FLIR TOOLS+ Software.

[66] Spain, Royal Decree 314/2006 Approving the Spanish Technical Building Code CTE-DB-HE1, 2006. Available at: http://www.boe.es/boe/dias/2006/03/28/pdfs/A11816-11831.pdf (Accessed 04 December 2016).

POSTPRINT

[67] J.M. Pérez -Bella, J. Domínguez-Hernández, E. Cano -Suñén, J.J. del Coz-Díaz, F.P. Álvarez Rabanal. A correction factor to approximate the design thermal conductivity of building materials. Application to Spanish façades. Energy Build. 88 (2015) 153–164.

[68] International Organization for Standardization, ISO/IEC Guide 98-3:2008. Uncertainty of Measurement. Part 3: Guide to the Expression of Uncertaintyin Measurement (GUM:1995), 1998, 2008.

[69] M. Gangolells, M. Casals. Resilience to increasing temperatures: residential building stock adaptation through codes and standards. Build. Res. Inf. 40(2012) 645–664.

[70] Spain, Royal Decree 2429/1979 Approving the Basic Building Norm on Thermal Conditions in Buildings NBE-CT-79, 1979, Available at: https://www.boe.es/boe/dias/1979/10/22/pdfs/A24524-24550.pdf (Accessed 04 December 2016).

[71] M. Gangolells, M. Casals, N. Forcada, M. Macarulla, E. Cuerva, Energy mappingof existing building stock in Spain, J. Clean. Prod. 112 (2016) 3895–3904.

[72] C. Peng, Z. Wu. In situ measuring and evaluating the thermal resistance of building construction. Energy Build. 40 (2008) 2076–2082.

[73] International Organization for Standardization, UNE EN ISO 10456:2012 (ISO10456:2007). Building materials and products – Hygrothermal properties- Tabulated design values and procedures for determining declared and design thermal values, 2012.

POSTPRINT